JOM 23691

Coordination chemistry of $[C(PPh_2)(P(S)Ph_2)_2]^-$: ^{31}P NMR of rhodium, iridium and platinum complexes, and the crystal and molecular structures of $[Rh(cod)\{C(PPh_2)(P(S)Ph_2)_2\text{-}P,S\}] \cdot CH_2Cl_2$ and $[RhI_2({}^tBuNC)_2\{C(PPh_2)(P(S)Ph_2)_2\text{-}P,S\}]$

Jane Browning, Keith R. Dixon, Neil J. Meanwell and Fang Wang

Department of Chemistry, University of Victoria, P.O. Box 3055, Victoria, B.C. V8W 3P6 (Canada)

(Received December 4, 1992)

Abstract

Complexes of the anionic ligand, $[C(PPh_2)(P(S)Ph_2)_2]^-$, are readily prepared under mild conditions by reactions of $CH(PPh_2)(P(S)Ph_2)_2$, in the presence of base ($NHEt_2$), with chlorobridged complexes, $[M_2Cl_2(cod)_2]$, M = Rh or Ir, cod = cycloocta-1,5-diene, $[Pt_2Cl_4(PEt_3)_2]$, and $[Pt_2Cl_2(MeOcod)_2]$, MeOcod = 8-methoxy-cyclooct-4-ene-1-yl. The products are $[M(cod)\{C(PPh_2)(P(S)Ph_2)_2\text{-}P,S\}]$, $[PtCl(PEt_3)\{C(PPh_2)(P(S)Ph_2)_2\text{-}P,S\}]$, and $[Pt(MeOcod)\{C(PPh_2)(P(S)Ph_2)_2\text{-}P,S\}]$ respectively, and the platinum complexes are both mixtures of the two possible isomers. Subsequent reactions of $[Rh(cod)\{C(PPh_2)(P(S)Ph_2)_2\text{-}P,S\}]$ with ^{t}BuNC followed by oxidative addition of I_2 or benzyl bromide give $[Rh({}^tBuNC)_2\{C(PPh_2)(P(S)Ph_2)_2\text{-}P,S\}]$, and isomeric mixtures of $[RhI_2({}^tBuNC)_2\{C(PPh_2)(P(S)Ph_2)_2\text{-}P,S\}]$ and $[RhBr(Bz)({}^tBuNC)_2\{C(PPh_2)(P(S)Ph_2)_2\text{-}P,S\}]$.

The complexes were characterized primarily by ^{31}P nuclear magnetic resonance (NMR) studies and by two crystal structure determinations. Complex **1a**, $[Rh(cod)\{C(PPh_2)(P(S)Ph_2)_2\text{-}P,S\}] \cdot CH_2Cl_2$ crystallized in the $P2_1/c$ (No. 14) space group ($Z = 4$) with $a = 12.294(3)$, $b = 16.063(5)$, $c = 21.384(5)$ Å, $\beta = 91.60(3)°$. Complex **4a(i)**, $[RhI_2({}^tBuNC)_2\{C(PPh_2)(P(S)Ph_2)_2\text{-}P,S\}]$ crystallizes in the $P\bar{4}2_1/c$ (No. 114) space group ($Z = 8$) with $a = b = 30.174(3)$, $c = 11.317(2)$ Å. Both complexes contain bidentate *P, S* bonded ligands with the second P=S group non-coordinated ("dangling"). In **1a**, approximate square planar coordination about rhodium is completed by the two double bonds of a cod ligand, and in **4a(i)**, the *P,S* ligand and two *cis* iodides comprise the equatorial plane of an octahedron which is completed by two ^{t}BuNC ligands.

1. Introduction

Tripodal anions are a rather rare class of ligands. The best known examples are the tris(pyrazolyl)borates, originally established by the work of Trofimenko [1,2] but still an area of active research [3]. Recently, phosphine chalcogenides such as $[C(P(S)Ph_2)_3]^-$ (and more generally $[C(P(X)Ph_2)(P(Y)Ph_2)(P(Z)Ph_2)]^-$, where the substituents, X, Y, and Z, can be simply electron pairs or the chalcogens, O, S, or Se) have been shown to have similar potential [4–11]. Several complexes exhibit tridentate (tripodal) *S,S,S*-coordination, for example in $[HgCl\{C(P(S)Me_2)(P(S)Ph_2)_2\text{-}S,S,S\}]$ [6] and $[Ag(PBu_3)\{C(P(S)Ph_2)_3\text{-}S,S,S\}]$ [8], but a bidentate *S,S*-coordination mode is also known in $[PtCl(PEt_3)\{C(P(S)Ph_2)_3\text{-}S,S\}]$ [10], $[Rh(cod)\{C(P(S)Ph_2)_3\text{-}S,S\}]$ [11], and $[Ir(CO)_2\{C(P(S)Ph_2)_3\text{-}S,S\}]$ [11]. In solution the bidentate complexes often show fluxional behaviour in which the non-coordinated P=S group exchanges rapidly with one or both of the coordinated P=S groups [10,11].

Additional recent impetus for this research area has been provided by the observation that these ligands may promote catalytic activity at some metal centres. Thus, $[C(P(O)Ph_2)_3]^-$ complexes of iridium are active hydrosilylation catalysts [12,13], and the tris(pyrazolyl)borate complex, $[Rh(CO)(C_2H_4)(HB(pz)_3)]$, is known to activate C–H bonds in benzene [3]. The fluxional behaviour may be germane to this activity, since during this reaction the trispyrazolylborate ligand changes from an initial η^2 to η^3 coordination in the product $[Rh(CO)H(Ph)\{HB(pz)_3\}]$.

Correspondence to: Professor K.R. Dixon.

0022-328X/93/$6.00

In $[Rh(cod)\{C(P(S)Ph_2)_3\text{-}S,S\}]$, the fluxional exchange process involves interchange of all three P=S groups [11], whereas in $[PtCl(PEt_3)\{C(P(S)Ph_2)_3\text{-}S,S\}]$, only the P=S group coordinated *trans* to PEt_3 participates in the fluxional exchange with the non-coordinated P=S group [10]. Thus, in the latter case, the process is essentially controlled by the Pt–S bond *trans* to Cl acting as a pivot for the exchange. The related complex, $[PtCl(PEt_3)\{C(P(S)Ph_2)_2\text{-}C,S\}]$ is different in that the ligand is coordinated via carbon, but exhibits a similar dynamic process in which exchange of the P=S groups is controlled by a Pt–C pivot [14,15]. In order to study the further possibility that a Pt–P bond might also serve as a pivot for related exchange processes, we have initiated a study of complexes of $CH(PPh_2)(P(S)Ph_2)_2$ and $[C(PPh_2)(P(S)Ph_2)_2]^-$. In the present paper we describe our preliminary studies of complexes of the anion, which are non-fluxional, and in a subsequent paper we will describe complexes of the neutral ligand, some of which exhibit the desired fluxionality.

2. Experimental section

2.1. Synthesis and spectroscopic studies

Data relating to the characterization of the complexes are given in the Tables, the Results section and in the preparative descriptions below. Microanalyses were performed by the Canadian Microanalytical Service, Vancouver, B.C., Canada. Infrared spectra were recorded in KBr disks from 4000 to 200 cm^{-1} with accuracy ± 3 cm^{-1} on a Perkin-Elmer 1320 grating spectrophotometer calibrated against polystyrene film. ^{31}P and ^{195}Pt NMR spectra were recorded in dichloromethane solution at 101.3 and 53.5 MHz respectively, using a Bruker WM250 Fourier transform spectrometer. Protons were decoupled by broad band ("noise") irradiation, and a lock signal was derived from the deuterium resonance of a capillary insert containing C_6D_6. ^{31}P chemical shifts were measured relative to external $P(OMe)_3$ and are reported in parts per million relative to 85% H_3PO_4 using a conversion factor of +141 ppm. ^{195}Pt chemical shifts are reported in ppm relative to $\Xi(^{195}Pt) = 21.4$ MHz. For both nuclei, positive chemical shifts are downfield of the reference.

All operations were carried out at ambient temperature (*ca.* 25°C) under an atmosphere of dry nitrogen using standard Schlenk tube techniques. Solvents were dried by reflux over appropriate reagents (calcium hydride for dichloromethane, and potassium/benzophenone for diethyl ether, toluene, and hexane) and were distilled under nitrogen prior to use. Recrystallization from solvent pairs were performed by dissolution of the complex in the first solvent (using about double the volume required for complete solution) followed by dropwise addition of sufficient second solvent to cause turbidity at ambient temperature. Crystallization was then completed either by continued very slow dropwise addition of the second solvent or by setting the mixture aside at a reduced temperature.

The ligand $CH(PPh_2)(P(S)Ph_2)_2$ [16], and the metal complexes, $[M_2Cl_2(cod)_2]$, M = Rh or Ir [17,18], $[Pt_2Cl_4(PEt_3)_2]$ [19], and $[Pt_2Cl_2(MeOcod)_2]$ [20] were prepared as previously described.

2.1.1. $[Ir(cod)\{C(PPh_2)(P(S)Ph_2)_2\text{-}P,S\}] \cdot CH_2Cl_2$

$CH(PPh_2)(P(S)Ph_2)_2$ (0.19 g, 0.30 mmol) was added to a stirred solution of $[Ir_2Cl_2(cod)_2]$ (0.10 g, 0.15 mmol) in dichloromethane (10 ml). Diethylamine (0.2 ml) was added. After 10 min the solvent was removed *in vacuo* and the residue extracted with toluene (20 ml). Solvent was removed from the extract *in vacuo* and the resulting residue recrystallized from dichloromethane/hexanes to give $[Ir(cod)\{C(PPh_2)(P(S)Ph_2)_2\text{-}P,S\}] \cdot CH_2Cl_2$ as orange crystals (0.18 g, 0.18 mmol). Anal. Calcd. for $C_{46}H_{44}Cl_2P_3S_2Ir$: C, 54.3; H, 4.36. Found: C, 54.1; H, 4.43%.

2.1.2. $[Rh(cod)\{C(PPh_2)(P(S)Ph_2)_2\text{-}P,S\}] \cdot CH_2Cl_2$

This complex was prepared by a procedure similar to that used above for the iridium analogue. $[Rh(cod)\{C(PPh_2)(P(S)Ph_2)_2\text{-}P,S\}] \cdot CH_2Cl_2$ was obtained as yellow crystals in 80% yield. Anal. Calcd. for $C_{46}H_{44}Cl_2P_3S_2Rh$: C, 59.6; H, 4.78. Found: C, 59.9; H, 5.55%.

2.1.3. $[Rh(^tBuNC)_2\{C(PPh_2)(P(S)Ph_2)_2\text{-}P,S\}] \cdot CH_2Cl_2$

A solution of ^{t}butylisocyanide (0.2 g, 2.4 mmol) in dichloromethane (2 ml) was added dropwise to a stirred solution of $[Rh(cod)\{C(PPh_2)(P(S)Ph_2)_2\}]$ (1.00 g, 1.08 mmol) in dichloromethane (50 ml). After 5 min the solvent was removed *in vacuo* and the residue crystallized by layering a dichloromethane solution with hexanes to give $[Rh(^tBuNC)_2\{C(PPh_2)(P(S)Ph_2)_2\text{-}P,S\}] \cdot CH_2Cl_2$ as yellow crystals (0.76 g, 0.77 mmol). Anal. Calcd. for $C_{48}H_{50}Cl_2N_2P_3S_2Rh$: C, 58.5; H, 5.11. Found: C, 59.0; H, 5.18%. IR: ν(CN) 2140s, 2100s, 2070sh cm^{-1}.

2.1.4. $[RhI_2(^tBuNC)_2\{C(PPh_2)(P(S)Ph_2)_2\text{-}P,S\}]$

A solution of diiodine (0.060 g, 0.24 mmol) in toluene (5 ml) was added dropwise to a solution of $[Rh(^tBuNC)_2\{C(PPh_2)(P(S)Ph_2)_2\text{-}P,S\}]$ (0.212 g, 0.24 mmol) in toluene (10 ml) and dichloromethane (5 ml) at −60°C. After 5 min the solution was warmed for a further 5 min to ambient temperature giving an initial mixture which contained at least three isomers (^{31}P NMR). After stirring for 4 h, a stable mixture of two isomers was obtained. Solvent was removed *in vacuo*, and the residue recrystallized from dichloromethane/hexanes to give $[RhI_2(^tBuNC)_2\{C(PPh_2)(P(S)Ph_2)_2$-*P,S*$\}]$ as red crystals (0.080 g, 0.069 mmol, isomer **4b(i)**). Anal. Calcd. for $C_{47}H_{48}I_2N_2P_3S_2Rh$: C, 48.9; H, 4.19. Found: C, 48.4; H, 4.17%. IR: ν(CN) 2175s cm^{-1}. A second isomer, **4a(x)**, was present in the supernatant from the recrystallization.

2.1.5. $[RhBr(CH_2Ph)(^tBuNC)_2\{C(PPh_2)(P(S)Ph_2)_2$-P,S$\}]$

A solution of benzyl bromide (0.012 ml, 0.10 mmol) in dichloromethane (1 ml) was added dropwise to a solution of $[Rh(^tBuNC)_2\{C(PPh_2)(P(S)Ph_2)_2$-*P,S*$\}]$ (0.087 g, 0.10 mmol) in dichloromethane (10 ml). A ^{31}P NMR spectrum recorded almost immediately showed the single isomer **4b(x)** (Table 1). After 10 min a second isomer, **4b(y)**, was found to be present. Removal of solvent *in vacuo*, followed by recrystallization of the residue from dichloromethane/diethyl ether gave crystalline **4b(x)**, with **4b(y)** in the supernatant. Alternatively, addition of a few drops of methanol to the mixture gave complete conversion to **4b(y)**, but in neither case could crystals of sufficient quality for elemental analysis be isolated.

2.1.6. $[PtCl(PEt_3)\{C(PPh_2)(P(S)Ph_2)_2$-P,S$\}]$

$CH(PPh_2)(P(S)Ph_2)_2$ (0.27 g, 0.42 mmol) was added to a stirred solution of $[Pt_2Cl_4(PEt_3)_2]$ (0.16 g, 0.21 mmol) in dichloromethane (5 ml). Diethylamine (0.2 ml) was added. After 5 min the solvent was removed *in vacuo* and the residue extracted with benzene (10 ml). Solvent was removed from the extract *in vacuo* and the resulting residue recrystallized from dichloromethane/diethyl ether to give $[PtCl(PEt_3)\{C(PPh_2)(P(S)Ph_2)_2$-*P,S*$\}]$ as yellow crystals (0.33 g, 0.34 mmol). Anal. Calcd for $C_{43}H_{45}ClP_4S_2Pt$: C, 52.7; H, 4.63. Found: C, 52.0; H, 4.48%. The product contained both isomers **2(i)** and **2(ii)** in about a 10:1 ratio.

2.1.7. $[Pt(MeOcod)\{C(PPh_2)(P(S)Ph_2)_2$-P,S$\}]$

$CH(PPh_2)(P(S)Ph_2)_2$ (0.17 g, 0.27 mmol) was added to a stirred solution of $[Pt_2Cl_2(MeOcod)_2]$ (0.10 g, 0.14 mmol) in dichloromethane (5 ml). Diethylamine (0.2 ml) was added. After 5 min the solvent was removed *in vacuo* and the residue extracted with toluene (5 ml). Solvent was removed from the extract *in vacuo* and the resulting residue recrystallized from dichloromethane/hexanes to give $[Pt(MeOcod)\{C(PPh_2)(P(S)Ph_2)_2$-*P,S*$\}]$ as colourless crystals (0.10 g, 0.10 mmol) characterized by ^{31}P and ^{195}Pt NMR spectroscopy. Isomers **3(i)** and **3(ii)** were present in about a 3:2 ratio. Attempts at recrystallization resulted in progressive decomposition so that we were unable to obtain good analytical data.

2.2. X-Ray data collection

Compounds **1a**, $[Rh(cod)\{C(PPh_2)(P(S)Ph_2)_2$-*P,S*$\}]\cdot CH_2Cl_2$ and **4a(i)**, $[RhI_2(^tBuNC)_2\{C(PPh_2)(P(S)Ph_2)_2$-*P,S*$\}]$, were prepared as described above and crystals suitable for study by X-ray diffraction were grown by vapour diffusion of hexanes into solutions of the complexes in dichloromethane.

TABLE 1. ^{31}P NMR parameters for complexes of L: $[C(P_CPh_2)(P_{A,B}(S)Ph_2)_2]^-$

Compound	Isomer	$\delta(P_A)$	$\delta(P_B)$	$\delta(P_C)$	$J(P_A-P_B)$	$J(P_A-P_C)$	$J(P_B-P_C)$	$J(M-P_A)$	$J(M-P_B)$	$J(M-P_C)$
Rh(cod)L	**1a**	56.0	42.3	39.5	46	115	20	nr	11	134
Ir(cod)L	**1b**	65.6	41.7	36.3	47	112	15			
$Rh(^tBuNC)_2L$	**1c**	63.7	41.8	50.8	44	132	16	nr	10	115
$RhI_2(^tBuNC)_2L$	**4a(i)**	67.1	39.6	52.2	33	87	11	nr	7	92
$RhI_2(^tBuNC)_2L$	**4a(x)**	65.3	37.1	51.0	27	87	nr	nr	nr	91
$RhBrBz(^tBuNC)_2L$	**4b(x)**	60.5	39.6	51.7	29	103	nr	nr	nr	93
$RhBrBz(^tBuNC)_2L$	**4b(y)**	65.1	41.0	52.3	32	92	nr	nr	nr	96
$PtCl(PEt_3)L$ [a]	**2(i)**	53.2	40.3	24.5	26	76	nr	27 [b]	225	3623
$PtCl(PEt_3)L$ [c]	**2(ii)**	62.8	43.2	34.6	43	110	nr	78	197	2200
Pt(MeOcod)L [d]	**3(i)**	58.1	42.5	29.6	38	88	8	57	245	3837
Pt(MeOcod)L [e]	**3(ii)**	67.2	45.0	35.7	51	143	20	109	116	1469

Isomer structures and atom labels are shown in Scheme 1. Unknown isomers are designated x or y. Spectra were recorded in dichloromethane solution with an external C_6D_6 lock. Chemical shifts (δ) are quoted in parts per million relative to 85% H_3PO_4. Coupling constants (J) are in Hz. nr = not resolved.

[a] $\delta(P_DEt_3)$ 8.3 ppm, $J(P_A-P_D)$ 6, $J(P_B-P_D)$ nr, $J(P_C-P_D)$ 10, $J(Pt-P_D)$ 3218 Hz. ^{195}Pt spectrum: $\delta(Pt)$ −9.1 ppm, $J(Pt-P_A)$ 27, $J(Pt-P_B)$ 225, $J(Pt-P_C)$ 3623, $J(Pt-P_D)$ 3221 Hz. [b] Not resolved in ^{31}P spectrum. Value obtained from ^{195}Pt spectrum. [c] $\delta(Pd_DEt_3)$ 15.3 ppm, $J(P_A-P_D)$ 43, $J(P_B-P_D)$ 12, $J(P_C-P_D)$ 423, $J(Pt-P_D)$ 2396 Hz. ^{195}Pt spectrum: $\delta(Pt)$ 62.0 ppm, $J(Pt-P_A)$ 78, $J(Pt-P_B)$ 197, $J(Pt-P_C)$ 2200, $J(Pt-P_D)$ 2396 Hz. [d] ^{195}Pt spectrum: $\delta(Pt)$ 208.6 ppm, $J(Pt-P_A)$ 56, $J(Pt-P_B)$ 245, $J(Pt-P_C)$ 3834 Hz. [e] ^{195}Pt spectrum: $\delta(Pt)$ 343.7 ppm, $J(Pt-P_A)$ *ca.* 112, $J(Pt-P_B)$ *ca.* 112, $J(Pt-P_C)$ 1468 Hz.

TABLE 2. Crystallographic data for **1a**, $[Rh(cod)\{C(PPh_2)(P(S)Ph_2)_2\text{-}P,S\}]\cdot CH_2Cl_2$, and **4a(i)**, $[RhI_2(^tBuNC)_2\{C(PPh_2)(P(S)Ph_2)_2\text{-}P,S\}]$.

	1a	4a(i)
formula	$C_{46}H_{44}Cl_2P_3S_2Rh$	$C_{47}H_{48}I_2N_2P_3S_2Rh$
fw	927.7	1154.7
space group	$P2_1/c$(No 14)	$P\bar{4}2_1/c$(No 114)
a, Å	12.294(3)	30.174(3)
b, Å	16.063(5)	30.174(3)
c, Å	21.384(5)	11.317(2)
α, deg	90	90
β, deg	91.60(3)	90
γ, deg	90	90
V, Å^3	4221	10304
Z	4	8
diffractometer	Picker 4-circle	Enraf-Nonius CAD4
radiation (λ, Å)	Mo Kα (0.71069)	Cu Kα (1.542)
μ, cm^{-1}	6.89	17.38
transm factor range	0.90–0.93	
temperature, K	295	295
no of obs reflcns ($I > 3.0\ \sigma(I)$)	2915	1369
parameters refined	307	167
R	0.087	0.084
R_w	0.094	0.095

$w = 1/(\sigma^2(F)+0.001F^2)$; $\Delta = \|F_o| - |F_c\|$. $R = (\Sigma\Delta/\Sigma F_o)$; $R_w = (\Sigma w\Delta^2/\Sigma wF_o^2)^{1/2}$

Preliminary photographic work was carried out with Weissenberg and precession cameras using Cu Kα radiation. After establishment of symmetry and approximate unit cells the crystals were transferred to one of two diffractometers (Table 2) and the unit cells refined by least squares methods employing pairs of centering measurements. During the subsequent data collection there was no evidence of decomposition of any of the crystals.

The Picker 4-circle instrument was automated with a PDP11/10 computer and used a $\theta/2\theta$ step scan with 160 steps of 0.01° in 2θ, counting for 0.25 s per step. Background measurements were for 20 s at each end of the scan. Each batch of 50 reflections was preceded by the measurement of three standard reflections, and, after application of Lorentz and polarization factors, each batch was scaled to maintain the sum of the standards constant. Absorption corrections were applied by a numerical integration using a Gaussian grid and with the crystal shape defined by perpendicular distances to crystal faces from a central origin.

Measurements on the CAD4 diffractometer used the NRCCAD modification of the Enraf-Nonius program [21], and the "Profile" $\omega/2\theta$ scan developed by Grant and Gabe [22]. Three standard reflections were measured every hour to check crystal stability and three others were measured every 400 reflections to check crystal orientation. Lorentz and polarization factors were applied and the data were corrected for absorption using an empirical method based on the work of North *et al.* [23] as implemented in the CAD4 structure determination package.

2.3. Structure solution and refinement

The structures were solved and refined using the SHELX-76 program package [24] and illustrations were drawn using ORTEP [25]. The atomic scattering factors used were for neutral atoms, with corrections for anomalous dispersion [26]. The structures were solved by direct methods, developed by standard Fourier synthesis procedures using difference maps, and refined by the method of least squares minimizing $\Sigma w\Delta^2$ where $\Delta = \|F_o| - |F_c\|$. The weights were obtained from counting statistics using $w = 1/(\sigma^2(F) + 0.001F^2)$. The metal atoms, and all phosphorus, sulphur, chlorine and iodine atoms were treated anisotropically, as was the central carbon, C(1), of the P,S ligand in **1a**, and the carbons of the cod ligand, C(38–46), in **1a**. All other atoms were treated isotropically. Hydrogen atoms were not located and are not included in the refinements. For **4a(i)** the six phenyl groups were refined as rigid hexagons each with different group temperature factors, which are included in the refinement. The final difference maps had minima/maxima of −0.65/0.75 (**1a**) and −1.1/0.88 eÅ^{-3} (**4a(i)**), with no indication that any material had been overlooked.

3. Results and discussion

3.1. Synthesis

In the presence of base ($NHEt_2$), the ligand, $CH(PPh_2)(P(S)Ph_2)_2$, reacts smoothly under mild conditions with the chlorobridged complexes, $[M_2Cl_2(cod)_2]$, M = Rh or Ir, cod = cycloocta-1,5-diene, $[Pt_2Cl_4(PEt_3)_2]$, and $[Pt_2Cl_2(MeOcod)_2]$, MeOcod = 8-methoxy-cyclooct-4-ene-1-yl. Hydrogen chloride is eliminated and the products are complexes of the anion, $[C(PPh_2)(P(S)Ph_2)_2]^-$. When no base is present, reactions often result in mixtures of complexes of the anion with complexes of the neutral ligand, $CH(PPh_2)(P(S)Ph_2)_2$. In only a few cases can the complex of the neutral ligand be isolated suggesting that $CH(PPh_2)(P(S)Ph_2)_2$ may be intermediate in behaviour between $CH_2(PPh_2)(P(S)Ph_2)$ and $CH(P(S)\text{-}Ph_2)_3$. Complexes of the former are readily prepared and require strongly basic reagent such as sodium hydride for deprotonation [27,28], whereas the latter normally deprotonates during complex formation and relatively few complexes of the neutral ligand have been reported [11].

The structures revealed by NMR and X-ray study (below) show that all the complexes contain bidentate

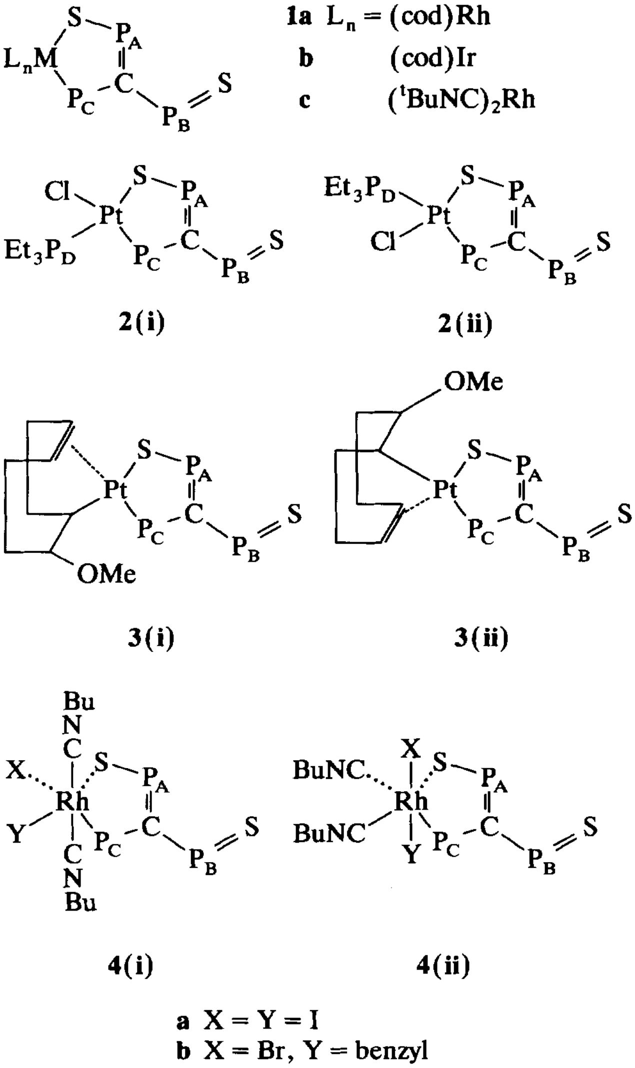

Scheme 1. Structures and atom labelling schemes for compounds 1–4. The two phenyl groups attached to each phosphorus have been omitted for clarity.

P,S coordinated ligands. There is no evidence for the *C,S* coordination mode found in [PtCl(PEt$_3$){CH(P(S)Ph$_2$)$_2$-*C,S*}] [14,15], an observation which is consistent with its non-occurrence in complexes of [CH(PPh$_2$)(P(S)Ph$_2$)]$^-$ [27,28]. Evidently, the presence of the strongly ligating PPh$_2$ group disfavours formation of the *C,S* bonded mode; although, in the present complexes, one would also expect steric crowding to be an obstacle to attachment of a metal at the central carbon. Thus, the [M(cod){C(PPh$_2$)(P(S)Ph$_2$)$_2$-*P,S*}], M = Rh or Ir, complexes have structure 1 (Scheme 1). For the platinum complexes, isomeric structures are possible for products derived from both [$Pt_2Cl_4(PEt_3)_2$] and [Pt_2Cl_2(MeOcod)$_2$]. In the former case ^{31}P NMR showed that the initial product is ca. 90% isomer **2(i)** with only about 10% **2(ii)**, and this contamination is further reduced by recrystallization. In the latter case the product ratio is *ca.* **3(i)**:**3(ii)** = 3:2, and separation was prevented by decomposition during recrystallization.

Oxidative addition reactions with this type of complex are of some interest because of the possibility of reactivity not only at the metal site but also at the methine carbon of the phosphine chalcogenide ligand [29]. Oxidative addition reactions to [Rh(cod){C(PPh$_2$)-(P(S)Ph$_2$)$_2$-*P,S*}] or its iridium analogue were inconclusive, resulting in partial reactions or complex isomer mixtures. More definitive results were achieved with [Rh(^{t}BuNC)$_2${C(PPh$_2$)(P(S)Ph$_2$)$_2$-*P,S*}], obtained by reaction of [Rh(cod){C(PPh$_2$)(P(S)Ph$_2$)$_2$-*P,S*}] with excess ^{t}butylisocyanide. The reactions are complicated by the multiple isomeric possibilities but [Rh(^{t}BuNC)$_2${C-(PPh$_2$)(P(S)Ph$_2$)$_2$-*P,S*}] with iodine leads ultimately to a crystalline product, [RhI$_2$(^{t}BuNC)$_2${C(PPh$_2$)(P(S)-Ph$_2$)$_2$-*P,S*}], isomer **4a(i)**. Overall, the possible isomers include the two *cis,trans* isomers **4a(i)** and **4a(ii)**, plus two enantiomeric pairs of *cis,cis* isomers; and **4a(i)** is not expected as the initial product since oxidative addition reactions normally show *trans* addition. Our initial reaction mixtures showed at least three different isomers with a stable mixture of two isomers developing over 4 h. Overlap of NMR lines prevented reliable assignments except for the latter two isomers. One of these is established as **4a(i)** by crystal structure determination. The other, labelled **4a(x)** in Table 1, is almost certainly not **4b(ii)** because ^1J(Rh–P$_C$) is very similar to the value in **4a(i)**. This would not be ex-

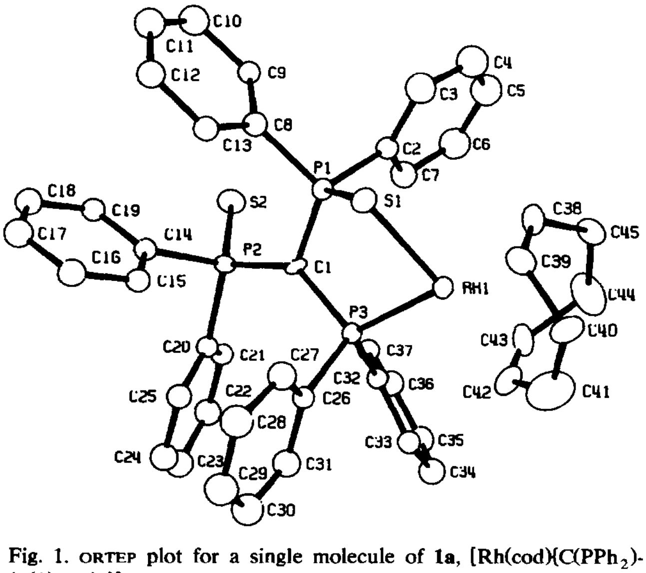

Fig. 1. ORTEP plot for a single molecule of **1a**, [Rh(cod){C(PPh$_2$)-(P(S)Ph$_2$)$_2$}].

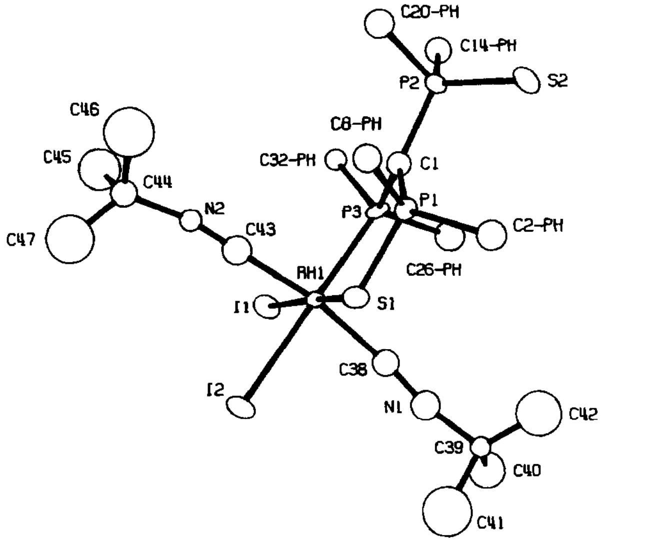

Fig. 2. ORTEP plot for a single molecule of **4a(i)**, $[RhI_2(^tBuNC)_2\{C(PPh_2)(P(S)Ph_2)_2\}]$.

pected with a change in the *trans* ligand from iodine to ^{t}BuNC and thus **4a(x)** is probably one of the *cis,cis* isomers with iodine *trans* to P_C.

Oxidative addition with an asymmetrical addend such as benzyl bromide is potentially even more complex, since, in addition to the four *cis,trans* isomers (**4b(i)**, **4b(i)** with X and Y interchanged, and **4b(ii)** plus its enantiomer), there are four enantiomeric pairs of *cis,cis* isomers. Addition of benzyl bromide to $[Rh(^tBuNC)_2\{C(PPh_2)(P(S)Ph_2)_2\text{-}P,S\}]$ gave two isomers, **4b(x)** and **4b(y)** (see Experimental section). Both gave ^{31}P NMR parameters (Table 1) which are similar to those of isomer **4a(i)** but it is not possible to make definitive structural assignments.

3.2. Nuclear magnetic resonance spectra

$^{31}P\{^1H\}$ nuclear magnetic resonance parameters for the complexes are collected in Table 1 (with $^{195}Pt\{^1H\}$ parameters in the Footnotes), and the atom labelling schemes are in Scheme 1. Basically the ^{31}P spectra are all simple first order patterns with three resonances for the $[C(PPh_2)(P(S)Ph_2)_2]^-$ ligand but the chemical shift assignments present problems. For example, the highest field resonance of $[Rh(cod)\{C(PPh_2)(P(S)Ph_2)_2\text{-}P,S\}]$ is a doublet (134 Hz) of doublets (115 Hz) of doublets (20 Hz) at 39.5 ppm. This is easily assigned to P_C, directly bonded to Rh, since the large 134 Hz coupling is not found elsewhere in the spectrum and is therefore due to $^1J(Rh\text{-}P_C)$. Assignment of the two remaining resonances, a doublet (115 Hz) of doublets (46 Hz) at 56.0 ppm and a doublet (46 Hz) of doublets (20 Hz) of doublets (11 Hz) at 42.3 ppm, presents an interesting dilemma. The most obvious assignment

TABLE 3. Fractional atomic coordinates and temperature parameters for **1a**, $[Rh(cod)\{C(PPh_2)(P(S)Ph_2)_2\}]\cdot CH_2Cl_2$

Atom	x	y	z	U_{eq}
Rh(1)	47081(10)	30511(9)	14635(6)	369(5)
S(1)	3972(3)	3204(3)	2465(2)	42(2)
S(2)	220(4)	4834(3)	1450(2)	47(2)
P(1)	2743(3)	3942(3)	2134(2)	34(2)
P(2)	625(3)	3647(3)	1455(2)	30(1)
P(3)	2938(3)	2869(3)	1062(2)	32(1)
C(1)	2035(11)	3457(9)	1520(7)	26(5)
C(2)	3369(13)	4919(10)	1941(8)	40(4)′
C(3)	4102(17)	5319(14)	2369(10)	72(6)′
C(4)	4632(18)	6055(15)	2199(11)	82(7)′
C(5)	4428(18)	6401(15)	1646(11)	85(7)′
C(6)	3690(18)	6074(14)	1203(11)	84(7)′
C(7)	3150(15)	5286(12)	1359(9)	60(5)′
C(8)	1948(13)	4176(11)	2811(8)	45(5)′
C(9)	1583(13)	4975(10)	2934(7)	40(4)′
C(10)	979(17)	5118(13)	3499(10)	71(6)′
C(11)	790(16)	4476(13)	3873(9)	67(6)′
C(12)	1120(15)	3662(12)	3774(9)	56(5)′
C(13)	1698(14)	3513(11)	3212(8)	45(5)′
C(14)	−49(12)	3084(10)	2091(7)	39(4)′
C(15)	341(13)	2295(10)	2266(8)	41(4)′
C(16)	−218(14)	1827(12)	2711(8)	55(5)′
C(17)	−1100(15)	2179(12)	2992(9)	60(5)′
C(18)	−1471(14)	2957(12)	2843(8)	54(5)′
C(19)	−936(13)	3445(10)	2378(8)	43(5)′
C(20)	14(12)	3125(10)	759(7)	37(4)′
C(21)	−324(13)	3630(10)	255(8)	42(4)′
C(22)	−841(14)	3267(12)	−274(8)	56(5)′
C(23)	−997(16)	2404(13)	−298(9)	64(6)′
C(24)	−654(15)	1905(12)	210(9)	60(5)′
C(25)	−121(14)	2277(11)	752(8)	48(5)′
C(26)	2568(12)	1758(9)	1095(7)	33(4)′
C(27)	2759(15)	1393(12)	1680(9)	58(5)′
C(28)	2457(17)	549(14)	1780(10)	77(6)′
C(29)	2017(17)	99(13)	1283(10)	73(6)′
C(30)	1871(17)	435(14)	705(10)	75(6)′
C(31)	2103(15)	1299(12)	602(9)	58(5)′
C(32)	2727(12)	3150(10)	236(7)	33(4)′
C(33)	3194(13)	2630(11)	−226(8)	45(5)′
C(34)	3106(15)	2876(12)	−863(9)	58(5)′
C(35)	2542(15)	3613(12)	−1012(9)	59(5)′
C(36)	2086(15)	4087(12)	−576(9)	58(5)′
C(37)	2192(13)	3869(10)	74(8)	42(4)′
C(38)	6212(13)	3666(12)	1812(9)	54(8)
C(39)	6338(14)	2833(13)	1917(9)	57(8)
C(40)	7010(16)	2222(13)	1506(10)	75(9)
C(41)	6539(22)	2028(23)	919(14)	164(18)
C(42)	5488(16)	2510(22)	672(11)	95(12)
C(43)	5412(20)	3326(20)	570(12)	90(11)
C(44)	6374(26)	3942(26)	668(11)	178(20)
C(45)	6698(19)	4168(14)	1287(8)	83(9)
C(46)	5329(25)	4458(27)	3989(19)	187(22)
Cl(1)	5960(8)	3533(6)	4185(5)	163(5)
Cl(2)	4056(9)	4500(7)	4244(5)	180(6)

Estimated standard deviations are given in parentheses. Coordinates $\times 10^n$ where $n = 5$ for Rh and 4 otherwise. Temperature parameters $\times 10^n$ where $n = 4$ for Rh and 3 otherwise. U_{eq} = the equivalent isotropic temperature parameter $= 1/3\, \Sigma_i \Sigma_j U_{ij} a_i^* a_j^* (\mathbf{a}_i \cdot \mathbf{a}_j)$. Primed values indicate that U_{iso} is given, where $T = \exp -(8\pi^2 U_{iso} \sin^2\theta / \lambda^2)$.

TABLE 4. Fractional atomic coordinates and temperature parameters for **4a(i)**, $[RhI_2(^tBuNC)_2\{C(PPh_2)(P(S)Ph_2)_2\}]$

Atom	x	y	z	U_{eq}
Rh(1)	2944(1)	4148(1)	2015(4)	33(2)
I(1)	3768(1)	4134(1)	2868(4)	57(2)
I(2)	3154(1)	3503(1)	393(4)	58(2)
S(1)	2228(4)	4147(5)	1183(16)	48(6)
S(2)	1415(5)	5422(5)	3946(17)	70(8)
P(1)	1906(4)	4672(5)	1828(15)	41(6)
P(2)	2023(5)	5493(5)	3336(16)	48(7)
P(3)	2718(5)	4702(4)	3336(13)	28(6)
N(1)	258(2)	332(2)	351(5)	8(2)′
N(2)	330(1)	480(1)	12(4)	3(1)′
C(1)	224(2)	499(2)	274(5)	5(2)′
C(2)	140(1)	441(1)	243(4)	7(1)′
C(3)	143(1)	416(1)	347(4)	7(1)′
C(4)	105(1)	397(1)	394(4)	7(1)′
C(5)	64(1)	402(1)	339(4)	7(1)′
C(6)	61(1)	427(1)	236(4)	7(1)′
C(7)	99(1)	447(1)	188(4)	7(1)′
C(8)	173(1)	503(1)	56(3)	5(1)′
C(9)	195(1)	498(1)	−52(3)	5(1)′
C(10)	183(1)	524(1)	−149(3)	5(1)′
C(11)	149(1)	555(1)	−138(3)	5(1)′
C(12)	127(1)	560(1)	−30(3)	5(1)′
C(13)	139(1)	534(1)	67(3)	5(1)′
C(14)	237(1)	576(1)	456(3)	6(1)′
C(15)	228(1)	568(1)	574(3)	6(1)′
C(16)	252(1)	589(1)	662(3)	6(1)′
C(17)	286(1)	618(1)	632(3)	6(1)′
C(18)	296(1)	626(1)	513(3)	6(1)′
C(19)	271(1)	605(1)	425(3)	6(1)′
C(20)	204(1)	591(1)	217(3)	7(1)′
C(21)	234(1)	588(1)	124(3)	7(1)′
C(22)	235(1)	621(1)	38(3)	7(1)′
C(23)	206(1)	657(1)	44(3)	7(1)′
C(24)	176(1)	659(1)	137(3)	7(1)′
C(25)	175(1)	627(1)	223(3)	7(1)′
C(26)	258(2)	447(1)	485(3)	8(1)′
C(27)	290(2)	420(1)	536(3)	8(1)′
C(28)	283(2)	402(1)	648(3)	8(1)′
C(29)	244(2)	410(1)	708(3)	8(1)′
C(30)	211(2)	437(1)	657(3)	8(1)′
C(31)	219(2)	456(1)	546(3)	8(1)′
C(32)	316(1)	510(1)	364(3)	3(1)′
C(33)	330(1)	536(1)	268(3)	3(1)′
C(34)	366(1)	564(1)	280(3)	3(1)′
C(35)	389(1)	566(1)	387(3)	3(1)′
C(36)	375(1)	540(1)	483(3)	3(1)′
C(37)	339(1)	512(1)	471(3)	3(1)′
C(38)	273(2)	363(2)	306(6)	6(2)′
C(39)	230(2)	300(2)	408(4)	3(1)′
C(40)	262(3)	280(3)	498(8)	11(3)′
C(41)	243(4)	257(4)	329(10)	20(5)′
C(42)	189(4)	315(4)	432(10)	19(4)′
C(43)	316(2)	457(2)	92(6)	7(2)′
C(44)	354(2)	503(2)	−77(5)	5(2)′
C(45)	393(3)	522(3)	−42(9)	15(4)′
C(46)	332(4)	541(4)	−96(10)	19(5)′
C(47)	374(4)	480(4)	−176(12)	21(5)′

Notes to Table 4:
Estimated standard deviations are given in parentheses. Coordinates $\times 10^n$ where $n = 4$ for Rh, I, S, P and 3 otherwise. Temperature parameters $\times 10^n$ where $n = 3$ for Rh, I, S, P and 2 otherwise. U_{eq} = the equivalent isotropic temperature parameter = $1/3\ \Sigma_i \Sigma_j U_{ij} a_i^* a_j^* (\mathbf{a}_i \cdot \mathbf{a}_j)$. Primed values indicate that U_{iso} is given, where $T = \exp - (8\pi^2 U_{iso} \sin^2\theta / \lambda^2)$.

would assume $^2J(Rh-P_A) > {}^3J(Rh-P_B)$ and place P_A at 42.3 and P_B at 56.0 ppm. However, this assumption leads to a number of inconsistencies in other assignments and with literature comparisons. For example, all the complexes in Table 1 contain a non-coordinated P=S group which should be relatively little affected by changes in the metal and associated ligands. The Table shows that it is the resonances *ca.* 40 ppm which remain relatively constant whereas the low field resonances vary widely (56–67 ppm). We thus prefer to assign the *ca.* 40 ppm resonances to P_B and the lower field resonances to P_A. This makes $^2J(Rh-P_A) < {}^3J(Rh-P_B)$ but such coupling patterns are not uncommon in heteronuclear situations. Although some ambiguity must remain, a number of other comparisons support our assignment:

1. The $\delta(P_B)$ values are similar to those for the P=S groups of $CH_2(PPh_2)(P(S)Ph_2)$ (40.4 ppm) [27], $CH(PPh_2)(P(S)Ph_2)_2$ (43.5 ppm) [7], $CH(P(S)Ph_2)_3$ (41.9 ppm) [7], and the non-coordinated P=S groups of $[PtCl(PEt_3)\{C(P(S)Ph_2)_3\text{-}S,S\}]$ (42.3 ppm) [10], and $[Rh(cod)\{C(P(S)Ph_2)_3\text{-}P,S\}]$ (42.3 ppm) [10], but markedly different from the shift of coordinated P=S in $[Rh(cod)\{CH(PPh_2)(P(S)Ph_2)\text{-}P,S\}]$ (54.2 ppm) [28].

2. δ_A and $^2J(P_A-P_C)$ for $[Rh(cod)\{C(PPh_2)(P(S)Ph_2)_2\text{-}P,S\}]$ (56.0 ppm, 115 Hz) are comparable to the values in $[Rh(cod)\{CH(PPh_2)(P(S)Ph_2)\text{-}P,S\}]$ (54.2 ppm, 121 Hz) [28]. Similarly, $[PtCl(PEt_3)\{C(PPh_2)(P(S)Ph_2)_2\text{-}P,S\}]$ (isomer **2(i)**: 53.2 ppm, 76 Hz; isomer **2(ii)**: 62.8 ppm, 110 Hz) may be compared with corresponding isomers of $[PtCl(PEt_3)\{CH(PPh_2)(P(S)Ph_2)\text{-}P,S\}]$ (*cis* isomer: 45.5 ppm, 81 Hz; *trans* isomer: 58.7 ppm, 117 Hz) [27].

3. With reference to the relative magnitudes of $^2J(M-P)$ and $^3J(M-P)$, we note that $^2J(Rh-P)$ was too small to resolve in $[Rh(cod)\{C(PPh_2)(P(S)Ph_2)\text{-}P,S\}]$ and related complexes [28]. Moreover, the known $^2J(Pt-P)$ values in the isomers of $[PtCl(PEt_3)\{CH(PPh_2)(P(S)Ph_2)\text{-}P,S\}]$ (42 and 50 Hz) [27] are comparable to the $J(Pt-P_A)$ values for $[PtCl(PEt_3)\{C(PPh_2)(P(S)Ph_2)_2\text{-}P,S\}]$ (27 and 78 Hz) and much smaller than the $J(Pt-P_B)$ values (225 and 197 Hz).

TABLE 5. Selected interatomic distances (Å)

1a, $[Rh(cod)\{C(PPh_2)(P(S)Ph_2)_2\}] \cdot CH_2Cl_2$		**4a**(i), $[RhI_2(^tBuNC)_2\{C(PPh_2)(P(S)Ph_2)_2\}]$	
Rh(1)–C(*x*)	2.05	Rh(1)–I(1)	2.668(5)
Rh(1)–C(*y*)	2.11	Rh(1)–I(2)	2.749(6)
Rh(1)–S(1)	2.361(4)	Rh(1)–S(1)	2.354(14)
Rh(1)–P(3)	2.336(4)	Rh(1)–P(3)	2.345(15)
Rh(1)–C(38)	2.21(2)	Rh(1)–C(38)	2.06(7)
Rh(1)–C(39)	2.23(2)	Rh(1)–C(43)	1.89(7)
Rh(1)–C(42)	2.15(2)		
Rh(1)–C(43)	2.16(2)		
S(1)–P(1)	2.032(6)	S(1)–P(1)	2.00(2)
S(2)–P(2)	1.971(6)	S(2)–P(2)	1.97(2)
P(1)–C(1)	1.74(2)	P(1)–C(1)	1.73(6)
P(1)–C(2)	1.80(2)	P(1)–C(2)	1.85(3)
P(1)–C(8)	1.81(2)	P(1)–C(8)	1.87(3)
P(2)–C(1)	1.76(1)	P(2)–C(1)	1.79(6)
P(2)–C(14)	1.85(2)	P(2)–C(14)	1.91(3)
P(2)–C(20)	1.85(2)	P(2)–C(20)	1.82(3)
P(3)–C(1)	1.77(1)	P(3)–C(1)	1.82(6)
P(3)–C(26)	1.84(2)	P(3)–C(26)	1.90(4)
P(3)–C(32)	1.83(2)	P(3)–C(32)	1.83(3)
		N(1)–C(38)	1.16(7)
		N(1)–C(39)	1.44(7)
		N(2)–C(43)	1.23(7)
		N(2)–C(44)	1.42(6)

C(*x*) and C(*y*) are the respective midpoints of the C(42)–C(43) and C(38)–C(39) double bonds. Estimated standard deviations are given in parentheses.

For the platinum complexes in Table 1, the ^{31}P spectra are somewhat complicated by the presence of ^{195}Pt sidebands (33.8% abundance). However, the simple first order ^{195}Pt spectra (doublet of doublets of doublets of doublets, 16 lines, for **2** and 8 line patterns for **3**) provide important confirmation of the assignments. For both **2** and **3** the isomers are assigned on the basis of *trans*-influence, assuming that the smaller

TABLE 6. Selected bond angles (°)

1a, $[Rh(cod)\{C(PPh_2)(P(S)Ph_2)_2\}] \cdot CH_2Cl_2$		**4a**(i), $[RhI_2(^tBuNC)_2\{C(PPh_2)(P(S)Ph_2)_2\}]$	
C(*x*)–Rh(1)–C(*y*)	87.1	I(1)–Rh(1)–I(2)	90.9(2)
C(*x*)–Rh(1)–P(3)	95.4	I(1)–Rh(1)–P(3)	92.9(4)
		I(1)–Rh(1)–C(38)	95(2)
		I(1)–Rh(1)–C(43)	86(2)
C(*y*)–Rh(1)–S(1)	89.1	I(2)–Rh(1)–S(1)	86.8(4)
		I(2)–Rh(1)–C(38)	86(2)
		I(2)–Rh(1)–C(43)	88(2)
S(1)–Rh(1)–P(3)	88.3(1)	S(1)–Rh(1)–P(3)	89.4(5)
		S(1)–Rh(1)–C(38)	86(2)
		S(1)–Rh(1)–C(43)	93(2)
		P(3)–Rh(1)–C(38)	95(2)
		P(3)–Rh(1)–C(43)	92(2)
Ph(1)–S(1)–P(1)	92.6(2)	Rh(1)–S(1)–P(1)	107.5(8)
S(1)–P(1)–C(1)	110.7(5)	S(1)–P(1)–C(1)	112(2)
Rh(1)–P(3)–C(1)	108.7(5)	Rh(1)–P(3)–C(1)	110(2)
		C(38)–N(1)–C(39)	165(6)
		C(43)–N(2)–C(44)	168(5)
P(1)–C(1)–P(2)	116.9(8)	P(1)–C(1)–P(2)	119(3)
P(1)–C(1)–P(3)	110.4(8)	P(1)–C(1)–P(3)	115(3)
P(2)–C(1)–P(3)	132.7(9)	P(2)–C(1)–P(3)	124(3)

C(*x*) and C(*y*) are the respective midpoints of the C(42)–C(43) and C(38)–C(39) double bonds. Estimated standard deviations are given in parentheses.

^1J(Pt–P) couplings are *trans* to Pt–P and Pt–C_σ bonds respectively.

3.3. X-Ray crystal structures

The atom labelling schemes and structures of single molecules of compounds **1a**, $[Rh(cod)\{C(PPh_2)(P(S)Ph_2)_2\text{-}P,S\}] \cdot CH_2Cl_2$, and **4a(i)**, $[RhI_2(^tBuNC)\{C(PPh_2)(P(S)Ph_2)_2\text{-}P,S\}]ClO_4 \cdot CH_2Cl_2$ are shown as ORTEP diagrams in Figs. 1 and 2 respectively. Unit cell and other parameters related to the crystal structure determinations are in Table 2. Fractional atomic coordinates and isotropic temperature parameters are given in Tables 3 and 4, and the most significant bond lengths and angles are collected in Tables 5 and 6. [30*].

In both structures, the ligand, $[C(PPh_2)(P(S)Ph_2)_2]^-$ is bidentate, coordinated via phosphorus and one sulphur, and with the second sulphur non-coordinated and over 6 Å away from rhodium. The geometries at C(1) are not consistent with tetrahedral carbon, clearly confirming deprotonation at this site. However, in each case there are significant distortions from trigonal planar geometry. The P–C–P bond angles are in the range 115–124° with the exception of P(2)–C(1)–P(3) in compound **1a** (133°), presumably due to steric crowding. Distortion is also evident in the geometry around C(1) in **4a(i)** except that here it causes C(1) to be 0.2 Å above the plane defined by P(1–3). Both of these distortions are readily seen in the ORTEP plots. The geometry around C(1) in **1a** is more closely planar with C(1) only 0.014 Å out of the P(1–3) plane. The bond lengths and angles within the *P,S* ligand systems of **1a** and **4a(i)** may be usefully compared with corresponding parameters in $[Rh(cod)\{C(P(S)Ph_2)_3\text{-}S,S\}]$ [11] and $[Rh(cod)\{C(PPh_2)(P(S)Ph_2)\text{-}P,S\}]$ [27]. For example the non-coordinated P=S bond lengths are all 1.97 Å, while the coordinated P=S groups lie in the range 2.00–2.04 Å. Rhodium–sulphur bond lengths are 2.34–2.36 Å; Rh–P, 2.30–2.35 Å; P–Rh–S angles 88.3–89.4°; and intra-ring P–C–P angles 110–16°. Other comparisons lie within similarly narrow ranges.

In compound **1a**, the coordination is closely square planar with inter-bond angles ranging from 87 to 95° and all ligating atoms within 0.04 Å of the least squares plane. In compound **4a(i)**, the two iodide ligands and the ligating atoms of the *P,S* ligand form an equatorial plane with inter-bond angles ranging from 87 to 93° and all atoms within 0.03 Å of the least squares plane. Octahedral coordination is completed by t-butylisocyanide ligands in axial positions. The interbond angles within the octahedron all lie in the range 86–95°.

* Reference number with an asterisk indicates a note in the list of references.

Acknowledgments

We thank the Natural Sciences and Engineering Research Council of Canada and the University of Victoria for research grants, Mrs K. Beveridge for technical assistance in the crystal structure determinations, and Mrs C. Greenwood for recording NMR spectra.

References and notes

1 S. Trofimenko, *Acc. Chem. Res.*, *4* (1971) 17.
2 S. Trofimenko, *Chem. Rev.*, *72* (1972) 497.
3 C.K. Ghosh, D.P.S. Rodgers and W.A.G. Graham, *J. Chem. Soc., Chem. Commun.*, (1988) 1511.
4 S.O. Grim and S.A. Sangokoya, *J. Chem. Soc., Chem. Commun.*, (1984) 1599.
5 S.O. Grim, S.A. Sangokoya, R.D. Gilardi, I.J. Colquhoun and W. McFarlane, paper presented at the 23rd International Conference on Coordination Chemistry, Boulder, CO, USA, 1984.
6 S.O. Grim, P.H. Smith, S. Nittolo, H.L. Ammon, L.C. Satek, S.A. Sangokoya, R.K. Khanna, I.J. Colquhoun, W. McFarlane and J.R. Holden, *Inorg. Chem.*, *24* (1985) 2889.
7 S.O. Grim, S.A. Sangokoya, I.J. Colquhoun, W. McFarlane and R.K. Khanna, *Inorg. Chem.*, *25* (1986) 2699.
8 S.O. Grim, S.A. Sangokoya, A.L. Rheingold, W. McFarlane, I.J. Colquhoun and R.D. Gilardi, *Inorg. Chem.*, *30* (1991) 2519.
9 S.O. Grim, P.B. Kettler and J.B. Thoden, *Organometallics*, *10* (1991) 2399.
10 J. Browning, K.A. Beveridge, G.W. Bushnell and K.R. Dixon, *Inorg. Chem.*, *25* (1986) 1987.
11 J. Browning, K.R. Dixon, R.W. Hilts, N.J. Meanwell and F. Wang, *J. Organomet. Chem.*, *410* (1991) 389.
12 R.S. Tanke and R.H. Crabtree, *J. Chem. Soc., Chem. Commun.*, (1990) 1056.
13 R.S. Tanke and R.H. Crabtree, *J. Am. Chem. Soc.*, *112* (1990) 7984.
14 J. Browning, G.W. Bushnell, K.R. Dixon and A. Pidcock, *Inorg. Chem.*, *22* (1983) 2226.
15 D.E. Berry, J. Browning, K.R. Dixon, R.W. Hilts and A. Pidcock, *Inorg. Chem.*, *31* (1992) 1479.
16 S.O. Grim, L.C. Satek and J.D. Mitchell, *Z. Naturforsch. B. Anorg. Chem. Org. Chem.*, *35* (1980) 832.
17 J.L. Herde, J.C. Lambert and C.V. Senoff, *Inorg. Synth.*, *15* (1974) 18.
18 G. Giordano and R.H. Crabtree, *Inorg. Synth.*, *19* (1979) 218.
19 J. Chatt and L.M. Venanzi, *J. Chem. Soc.*, (1955) 2787.
20 J. Chatt, L.M. Vallarino and L.M. Venanzi, *J. Chem. Soc.*, (1957) 2496.
21 Y. Le Page, E.J. Gabe and P.S. White, NRCCAD modification of the Enraf-Nonius program, Chemistry Division, National Research Council of Canada, Ottawa, Canada.
22 D.F. Grant and E.J. Gabe, *J. Appl. Cryst.*, *11* (1978) 114.
23 A.C.T. North, D.C. Phillips and F.S. Mathews, *Acta Crystallogr.*, *A24* (1968) 351.
24 G.M. Sheldrick, SHELX-76, *A Computer Program for Crystal Structure Determination*, University of Cambridge, UK, 1976.
25 C.K. Johnson, ORTEP, Report ORNL-3794, Oak Ridge National Laboratory, Oak Ridge, TN, USA, 1965.

26 D.T. Cromer and J.T. Waber, in J.A. Ibers and W.C. Hamilton (Eds.), *International Tables for X-ray Crystallography, Vol. IV*, Kynoch Press, Birmingham, 1974.
27 D.E. Berry, J. Browning, K.R. Dixon and R.W. Hilts, *Can. J. Chem., 66* (1988) 1272.
28 J. Browning, G.W. Bushnell, K.R. Dixon and R.W. Hilts, *J. Organomet. Chem., 452* (1993) 205.
29 J. Browning, K.R. Dixon and R.W. Hilts, *Organometallics, 8* (1989) 552.
30 Supplementary material have been deposited with the Cambridge Crystallographic Data Centre: For **1a** and **4a(i)**: unit cell, data collection and refinement parameters (Table S1), fractional atomic coordinates and isotropic temperature parameters for all atoms (Tables S2, S3), anisotropic temperature factors for all atoms (Tables S4, S5), interatomic distances (Tables S6, S7), bond angles (Tables S8, S9); selected intermolecular distances (Tables S10, S11); observed and calculated structure factor amplitudes (Tables S12, S13).